THE ALL-SKY AUTOMATED SURVEY FOR SUPERNOVAE (ASAS-SN) LIGHT CURVE SERVER V1.0

C. S. Kochanek[1,2], B. J. Shappee[3,4], K. Z. Stanek[1,2], T. W.-S. Holoien[1,2,8], Todd A. Thompson[1,2], J.-L. Prieto[5,6], Subo Dong[7], J. V. Shields[1], D. Will[1], C. Britt[9], D. Perzanowski[9], G. Pojmański[10]

Draft version June 21, 2017

ABSTRACT

The All-Sky Automated Survey for Supernovae (ASAS-SN) is working towards imaging the entire visible sky every night to a depth of $V \sim 17$ mag. The present data covers the sky and spans $\sim$ 2-5 years with $\sim$ 100-400 epochs of observation. The data should contain some $\sim$ 1 million variable sources, and the ultimate goal is to have a database of these observations publicly accessible. We describe here a first step, a simple but unprecedented web interface https://asas-sn.osu.edu/ that provides an up to date aperture photometry light curve for any user-selected sky coordinate. Because the light curves are produced in real time, this web tool is relatively slow and can only be used for small samples of objects. However, it also imposes no selection bias on the part of the ASAS-SN team, allowing the user to obtain a light curve for any point on the celestial sphere. We present the tool, describe its capabilities, limitations, and known issues, and provide a few illustrative examples.

Subject headings: surveys – stars:variables – stars:supernovae – quasars

1. INTRODUCTION

Paczyński (2000) outlined the astrophysical need for all-sky variability surveys and the desirability of public access. Well over a decade later, the All-Sky Automated Survey for Supernovae (ASAS-SN, Shappee et al. 2014) is the first to routinely survey the entire visible sky, reaching a depth of roughly 17 mag. ASAS-SN has publicly announced all transient detections from its inception. Here we take the first step towards making the data more publicly accessible, with a tool to allow astronomers to obtain a current light curve of an arbitrary point on the sky.

Many ground-based surveys have offered retrospective access to databases of light curves of varying depths and survey areas. The widest area examples are the original All-Sky Automated Survey (ASAS, Pojmanski 2002), the Northern Sky Variability Survey (NSVS, Woźniak et al. 2004), the Catalina Real-Time Survey (CRTS, Drake et al. 2009) and the Palomar Transient Factory (PTF, Law et al. 2009). Examples of smaller area surveys with publicly available light curves are the Optical Gravitational Lensing Experiment (OGLE, Udalski et al. 2008) and the Sloan Digital Sky Survey's

Stripe 82 (SDSS, Ivezić et al. 2007). For many of the brightest variables, the compilation of data from (primarily) amateur astronomers by the American Association of Variable Star Observers (AAVSO) remains the best public source of data.

As of mid-2017, ASAS-SN consists of two stations, located at the Haleakala Observatory (Hawaii) and the Cerro Tololo International Observatory (CTIO, Chile) sites. The stations are hosted by Las Cumbres Observatory (Brown et al. 2013), and are operated through their network. By the end of 2017, ASAS-SN will have five stations, with the addition of a second unit at CTIO and one each at McDonald Observatory (Texas), and the South African Astrophysical Observatory (SAAO, Sutherland, South Africa) sites. The new stations will also be hosted by Las Cumbres Observatory.

A station consists of four 14 cm aperture Nikon telephoto lenses, each with a thermo-electrically cooled, back-illuminated, 2048^2, Finger Lakes Instruments, Pro-Line CCD camera. The field of view of each camera is roughly 4.5 deg^2, the pixel scale is $8''0$, and the image FWHM is $\sim$ 2 pixels. With overlaps between observing fields, the instantaneous "field of view" with 5 stations will be roughly 360 square degrees. Observations are made using the V (original two stations) or g (three new stations) band filters and three dithered 90 sec exposures. Assuming an average 10 hour night, the system will be able to survey 48,000 square degrees per night by the end of 2017, with considerable robustness against weather losses thanks to the multiplicity of sites. The operations of ASAS-SN are presently funded through the end of 2021.

To date, ASAS-SN has focused on its primary, original goal of carrying out a survey for bright transients across the visible sky with minimal observational bias. This was particularly aimed at obtaining a complete inventory of nearby supernovae (SNe) to well characterize the local SN rate and its correlations with galaxy type and properties. The supernova search, cataloged in Holoien et al. (2017a,b,c), has led to a significant increase in the dis-

[1] Department of Astronomy, The Ohio State University, 140 West 18th Avenue, Columbus, OH 43210
[2] Center for Cosmology and Astroparticle Physics, The Ohio State University, 191 W. Woodruff Avenue, Columbus, OH 43210
[3] Carnegie Observatories, 813 Santa Barbara Street, Pasadena, CA 91101
[4] Hubble and Carnegie-Princeton Fellow
[5] Núcleo de Astronomía de la Facultad de Ingeniería y Ciencias, Universidad Diego Portales, Av. Ejército 441, Santiago, Chile
[6] Millennium Institute of Astrophysics, Santiago, Chile
[7] Kavli Institute for Astronomy and Astrophysics, Peking University, Yi He Yuan Road 5, Hai Dian District, China
[8] US Department of Energy Computational Science Graduate Fellow
[9] ASC Technology, College of Arts and Science, The Ohio State University, 125 S. Oval Mall, Columbus, OH 43235
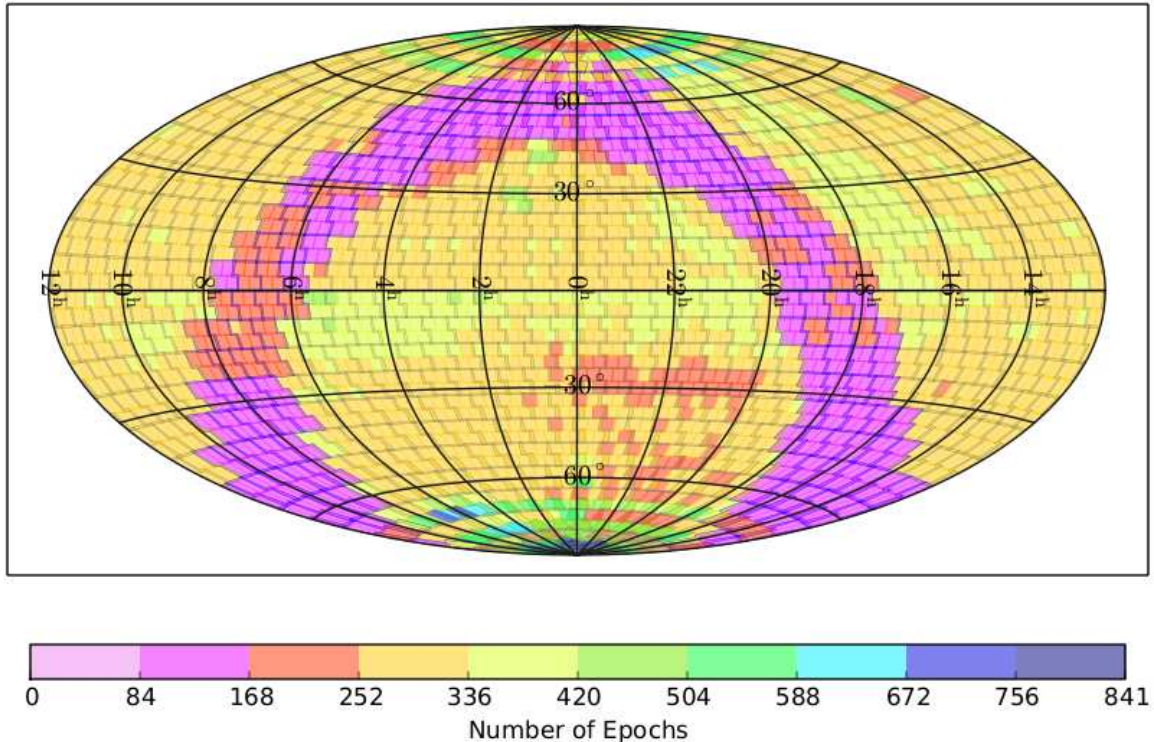[10] Warsaw University Observatory, Al Ujazdowskie 4, 00-478Warsaw, Poland

FIG. 1.— Equatorial projection of the number of available ASAS-SN epochs. There are some artifacts because of historical details as ASAS-SN built up to two complete stations. There are, on average, 2.6 images for each epoch.

covery rate of bright SNe while eliminating the bias of amateurs towards SNe in large galaxies. ASAS-SN is also finding many more SNe close to the cores of galaxies than other amateur and professional searches.

In the process of finding SNe, including the most luminous SN to date (ASASSN-15lh, Dong et al. 2016, Godoy-Rivera et al. 2017), many other transient sources have also been routinely discovered. The most common are cataclysmic variables (CVs), which are so numerous that they are simply released on a separate WWW page[11] and the light curves are available from the ASAS-SN CV Patrol[12] (Davis et al. 2015). ASAS-SN is the dominant source for reporting new CVs and CV outbursts (see, e.g., Kato et al. 2016). Rarer Galactic events are classical novae (e.g., Stanek et al. 2016), M and even L dwarf flares (e.g., Schmidt et al. 2014, 2016), and outbursts of young stellar objects (Holoien et al. 2014a, Herczeg et al. 2016). Rarer extragalactic events are tidal disruption events (TDEs), where the majority of the best studied TDEs have been discovered by ASAS-SN (Holoien et al. 2014b, 2016a,b, Brown et al. 2016, 2017a) or are present in ASAS-SN (Brown et al. 2017b), and "changing-look" AGN (Shappee et al. 2014).

ASAS-SN has not focused on other sources of variability to date, although the project has supplied light curves or variability searches for a range of other projects. For example, there are studies of "eclipsing" events (Rodriguez et al. 2016, Rodriguez et al. 2017, Osborn et al. 2017) and other (Gully-Santiago et al. 2017) properties of T Tauri stars. Littlefield et al.

(2016) examined the recovery of the intermediate polar FQ Aquarii from its low state in 2016. ASAS-SN observations were also used to limit any optical counterparts to high energy γ-ray (Abeysekara et al. 2015) and ICE-CUBE neutrino events (Aartsen et al. 2017). Internally, ASAS-SN has identified large numbers of previously unreported variable stars which will start being released in the near future.

As part of the next phase of ASAS-SN, the intent is to provide a steadily expanding set of tools for obtaining ASAS-SN light curves. The first version, released here, is a tool to obtain an ASAS-SN light curve of any user-selected position of the sky. It is a relatively slow tool since it simply carries out aperture photometry at the requested location, but it also involves no preconceptions on the part of ASAS-SN as to what represents an interesting source. Bulk light curve requests will not be possible with the current tool because the necessary computations are done on request – we invite anyone interested in large numbers of light curves to contact the ASAS-SN team. The next phase will be to build a database of the light curves of known variables and variables discovered by ASAS-SN, with the goal of having this tool available in 2018. The final phase will be to have a complete database of light curves for ASAS-SN sources. The staged releases will allow the ASAS-SN team to develop, test, and debug the releases in a logical and controlled order from the simple to the complex.

In §2 we describe the initial tool and present some examples of both its uses and its limitations. In §3 we provide a short summary. Research making use of these light curve tools either through direct use of the light curves or simply as a source for confirmations should cite

[11] http://www.astronomy.ohio-state.edu/~assassin/transients.html
[12] http://cv.asassn.astronomy.ohio-state.edu/

Shappee et al. (2014) for the ASAS-SN survey and this paper for the light curves.

2. ASAS-SN LIGHT CURVES

The requirement that we impose no restriction on the location at which a light curve can be obtained means that the light curves must be computed at the time of the request. This is a straightforward process, but slow compared to pre-computing light curves for a defined sample of sources and storing them in a database. As discussed in the introduction, such tools will be made available for ASAS-SN in the relatively near future.

Figures 1 and 2 summarize the number of epochs and the temporal span of the ASAS-SN data at the present time. On average there are 2.6 images per epoch, which is less than the nominal value of 3 because we initially used only 2 dithered images per epoch and weather and scheduling idiosyncrasies can lead to obtaining fewer than 3 good images. Most of the structures in the two Figures can be understood from the history by which ASAS-SN reached its current state with two stations each with four cameras. ASAS-SN started with the Hawaii station and two cameras (`ba` and `bb`) in early 2013, and it was expanded to four cameras (adding `bc` and `bd`) in (roughly) December 2013. The CTIO station was deployed with two cameras (`be` and `bf`) in May 2014 and expanded to four cameras (adding `bg` and `bh`) in July 2015.

Initially, we tried to observe the entire sky visible from Hawaii, but then dropped the Galactic plane and declinations $< -20°$ in order to increase the cadence for the extragalactic fields. As the system approached its current state, we resumed observing the Northern Galactic plane. Hence the time spanned by the data is relatively uniform above declination $-20°$, but there are fewer epochs along the plane. From CTIO, we initially avoided the Southern Galactic plane, but then began observing it somewhat after we resumed observing the Northern Galactic plane. The Magellanic Clouds, M 31 and M 33 are observed at a higher cadence. Most of the other smaller scale structures are minor artifacts from dealing with some shifts in field definitions as cameras were added. Under the present plan, the McDonald Observatory station will have cameras `bi-bl`, the SAAO station will have cameras `bm-bp`, and the second CTIO station will have cameras `bq-bt`. Images from the new stations will be incorporated into this tool after an initial period for testing.

The present tool, `https://asas-sn.osu.edu/`, takes as input a coordinate (RA/Dec) and a look-back time (days) and then provides a light curve for that position both as a graph and as a down-loadable table by doing aperture photometry on the individual ASAS-SN images. The look-back time is provided to allow the rapid extraction of the recent behavior of a target. Images taken in particularly poor conditions, that were out of focus ($FWHM > 2.5$ pixels), had poor astrometry, or where the source is within 0.2 deg of the detector edge are automatically rejected. The latter restriction opens no gaps in the sky coverage because of the 0.5 deg field overlaps. Photometry is simply extracted at the requested position, as there is no need for any re-centering step for the images with good astrometry. This also means that it is possible to obtain light curves for faint sources close to bright sources, making allowance for the effects of crowding (see below).

For the selected images, the photometry is done using the `IRAF apphot` package and calibrated using the AAVSO Photometric All-Sky Survey (APASS, Henden et al. 2012). The signal is taken from a 2 pixel radius aperture (i.e., about 2 FHWM in diameter) and the background is estimated in a 7 to 10-pixel radius annulus. The background pixels are clipped at 2σ. The aperture photometry is done both for the target position and 100 nearby $11.5 < V < 14$ mag APASS stars with photometric uncertainties less than 0.075 mag. The APASS magnitude range is chosen to avoid saturation and minimize crowding. The APASS stars are also required to have no other APASS star within $56''.25$ (about 3 ASAS-SN FWHM) in separation and 5 mag in flux.

The calibration is set by the median difference between the APASS and instrumental aperture magnitudes for each image after iteratively clipping the APASS calibration stars at a threshold where we would expect to lose one or fewer stars given Gaussian errors. We assume that any dispersion larger than 0.15 mag is dominated by outliers and use this as a maximum for the estimated dispersion. After clipping the calibration sample, the weighted mean is used as the final calibration. The returned light curve gives the HJD and UT dates of the observation, the camera name (`b?`), the FWHM (for monitoring any residual focus issues), the estimated 5σ detection limit for the location, the aperture magnitude and its uncertainty and the flux estimate and its uncertainty (in mJy). The aperture magnitude becomes the 5σ detection limit once it is below the detection limit. However, the fluxes are always the real flux measurements and their uncertainties and so can be easily combined across images even when the magnitude is only reported as a limit.

We illustrate the utility of ASAS-SN light curves with four examples of non-transient sources. In each case, these are the light curves for the individual exposures, and the multiple exposures for each epoch can be combined to reduce the uncertainties or improve the upper limits. We simply show the data as returned by the query. Figure 3 shows the ASAS-SN light curve of a classic example of a high amplitude variable star, R Coronae Borealis (R CrB). The light curve spans 7.3 mag and is well-defined even at its brightest points, where it is well above ASAS-SN's nominal saturation magnitude (see below). Figure 4 shows a much more subtle example, the phased light curve of the eclipsing binary M dwarfs KELT J041621−620046 (Lubin et al. 2017). This 1.11 day binary has a mean magnitude of $V \simeq 13.9$ and 0.3 mag eclipses that are easily seen in the ASAS-SN data. The outliers in Figure 4 can be eliminated by rejecting data with unusually large magnitude uncertainties. As a more distant example, Figure 5 shows the ASAS-SN light curve of HV 2112, a star in the Small Magellanic Cloud that Levesque et al. (2014) propose is a Thorne-Zytkow object (a red supergiant with a neutron star at its core). Finally, as an extragalactic example, Figure 6 shows the ASAS-SN light curve of the classic reverberation mapping target (most recently by De Rosa et al. 2015), NGC 5548. The variability of this AGN is well determined despite doing the photometry at the center of a resolved galaxy.

The two main issues the user should be aware of are crowding and saturation. The ASAS-SN light curves
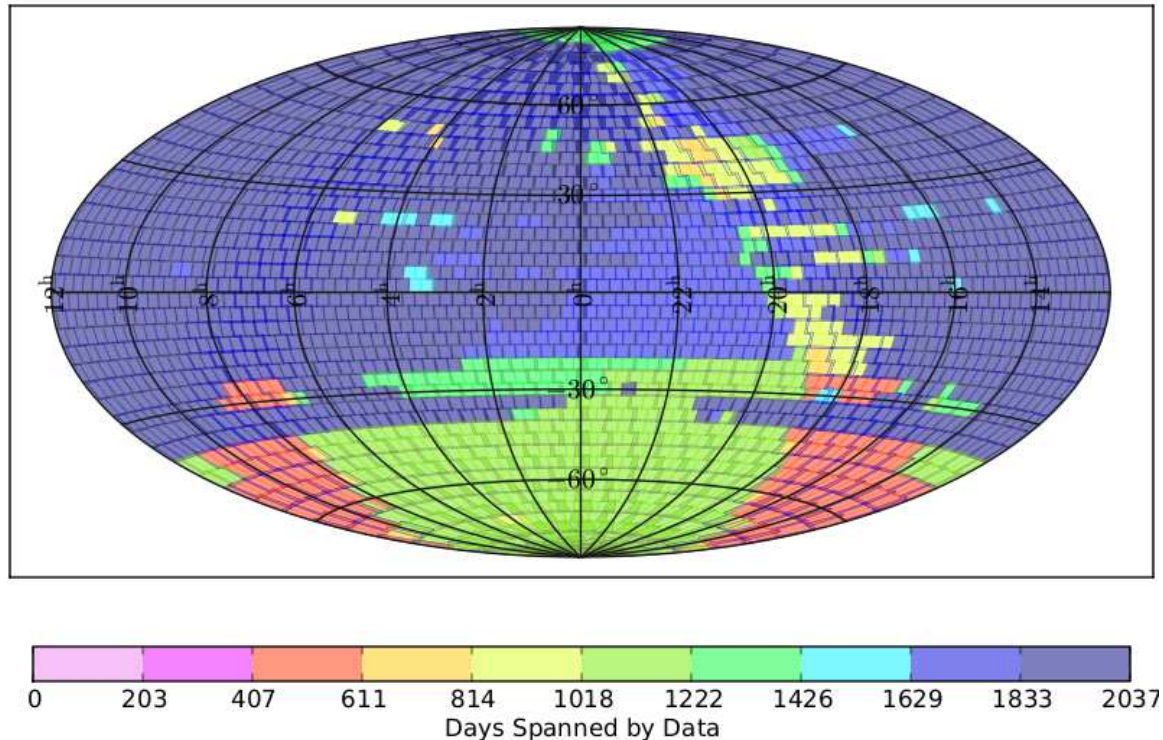
FIG. 2.— Equatorial projection of the time spanned by the ASAS-SN data. There are some artifacts because of historical details as ASAS-SN built up to two complete stations, and the temporal coverage of the (Northern) Galactic plane has a significant gap.

are fairly robust against both problems, provided they are neither pushed to extremes nor over-interpreted. To help visually evaluate both issues, the light curve server page returns an Aladin Sky Atlas (Bonnarel et al. 2000, Boch & Fernique 2014) image of the region surrounding the target. This also provides a visual confirmation of the selected target.

An example of crowding is the massive, eclipsing Wolf-Rayet binary WR20a (Bonanos et al. 2004). Figure 7 shows the ASAS-SN and DSS images of WR20a, where the circle around the source is $10\rlap{.}''0$ in radius. At the resolution of ASAS-SN, the local crowding will tend to change the light curve by some constant in flux, distorting its shape. Figure 8 shows the phased ASAS-SN light curve of WR20a, and we find that the eclipse depths are slightly underestimated (about 0.3 mag instead of 0.4 mag) because of the crowding. Since the ASAS-SN image FWHM are set by the camera optics rather than atmospheric seeing, there are essentially no effects equivalent to the light curve distortions produced by combining crowding with variable seeing. Despite the distortion of the light curve, there is no difficulty recognizing that the source is an eclipsing binary and determining the period. In fact, Figure 8 used the primary eclipse time of 2453124.569 from Bonanos et al. (2004) but a revised period of 3.684599 days because the original 3.686 ± 0.01 day estimate clearly led to small phasing errors.

ASAS-SN saturates at 10-11 mag, where the exact limit depends on the camera and the image position (vignetting). However, ASAS-SN uses a procedure inherited from the original ASAS survey (Pojmanski 2002) that moves flux out of the bleed trails of bright stars and back into the central image. After basic process-

ing, frames are scanned for saturated pixels. Once one is found, all connected saturated pixels and their associated edge effects are identified. The flux of the saturated pixels is then added back as a Gaussian around the centroid position. The regions from which the flux was removed are filled in by linear interpolation of the adjacent, unsaturated pixels.

To the extent that the charge bleeding process is conservative and the saturated star is relatively isolated, this leads to a substantial improvement in the photometry of saturated stars. We illustrate this in Figure 9 with the light curve of the $P = 18.9$ day Cepheid VY Car. There are clearly outliers and it would be unwise to use the photometry for determining the distance scale, but there is no difficulty recognizing the classic, long-period Cepheid light curve and determining its period and phase. There are also some clear patterns in the un-phased light curves that would allow the production of a clean light curve after some manual editing. This bright star correction procedure will not, however, salvage the light curves of the stars that lay underneath the bleed trails.

3. DISCUSSION

While https://asas-sn.osu.edu/ as V1.0 of ASAS-SN light curve servers is slow because the light curves must be computed upon request, it does provide the first astronomical resource able to provide an up to date light curve for any point on the celestial sphere upon demand. If the requested position is currently visible, the most recent epochs will generally be less than a week old even with weather interruptions. This service is not meant for obtaining large numbers of light curves, with requests being self-limiting by the allocated computational re-
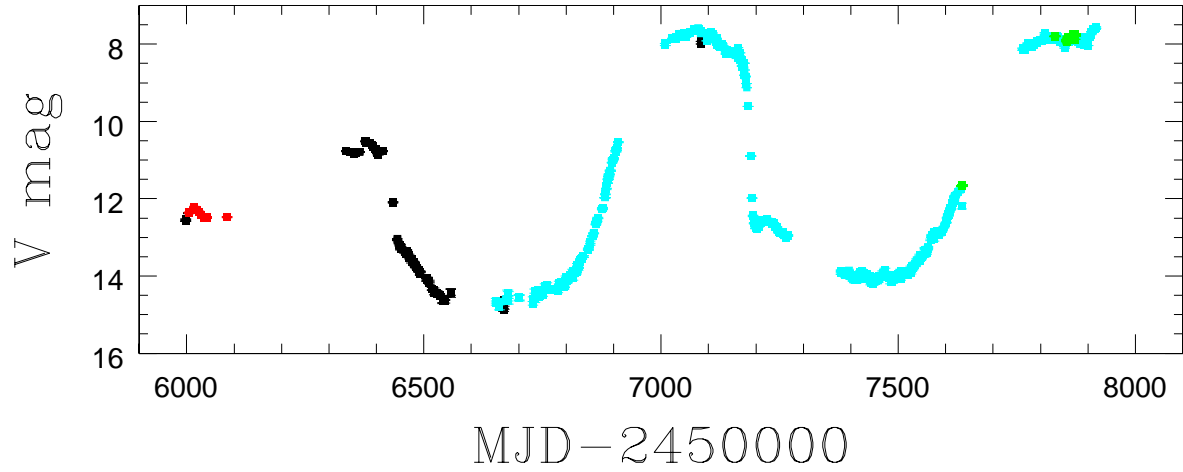
FIG. 3.— The ASAS-SN light curve of R Coronae Borealis. The different colors are data from different cameras.
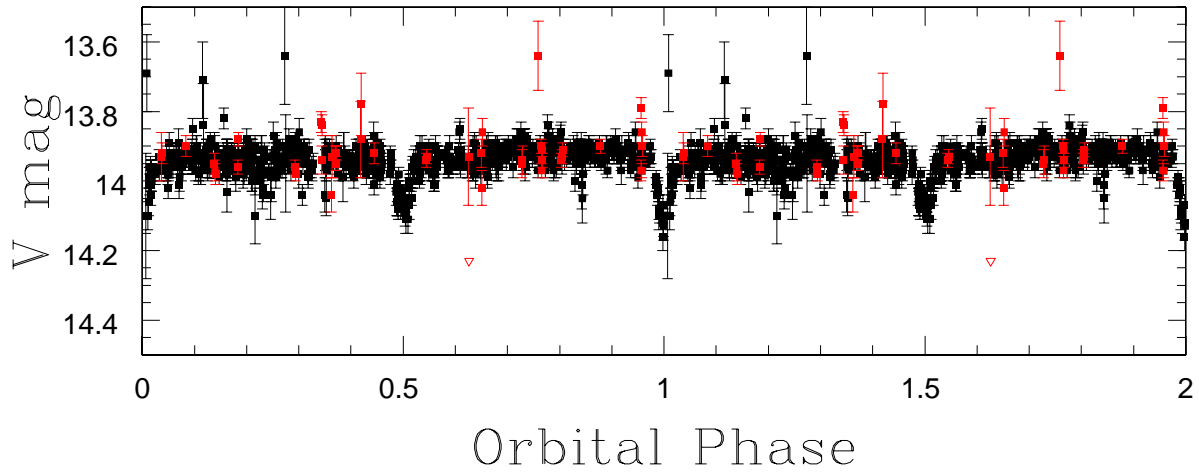

FIG. 4.— Phased ASAS-SN light curve of the eclipsing binary pair of M dwarfs KELT J041621−620046 (Lubin et al. 2017). The different colors are data from different cameras.
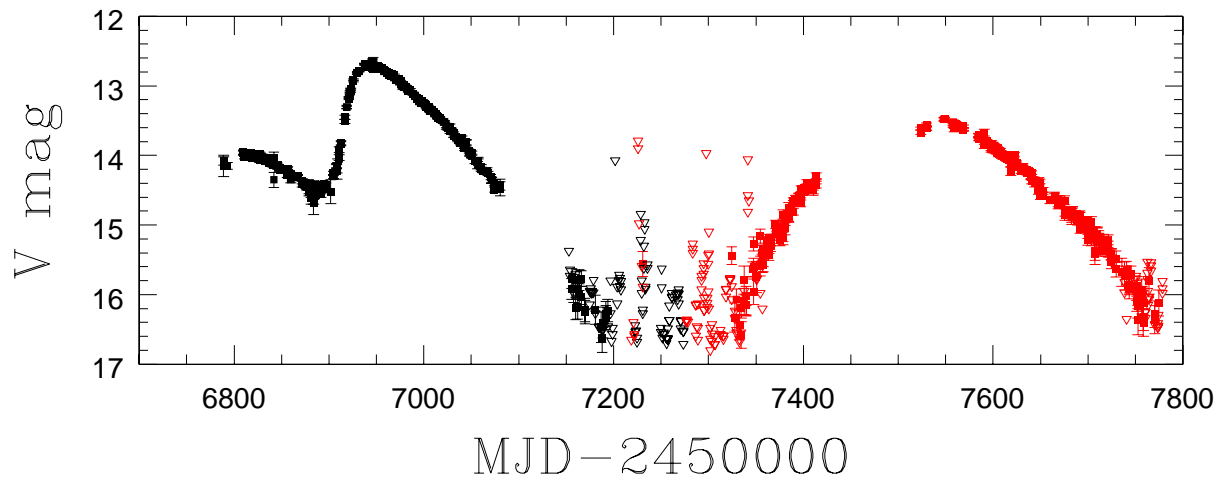

FIG. 5.— ASAS-SN light curve of the proposed Thorne-Zytkow object HV 2112 in the Small Magellanic Cloud (Levesque et al. 2014). Squares with error bars are detections and triangles are 5σ upper limits. The different colors are data from different cameras.
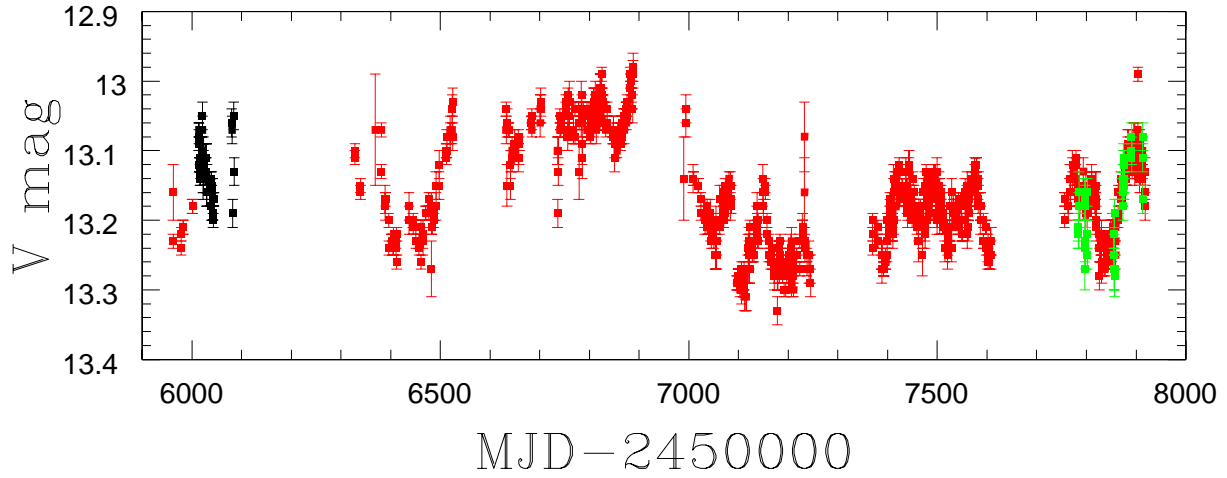
FIG. 6.— ASAS-SN light curve of the AGN NGC 5548. One anomalous point falls below the bottom of the figure. The different colors are data from different cameras.
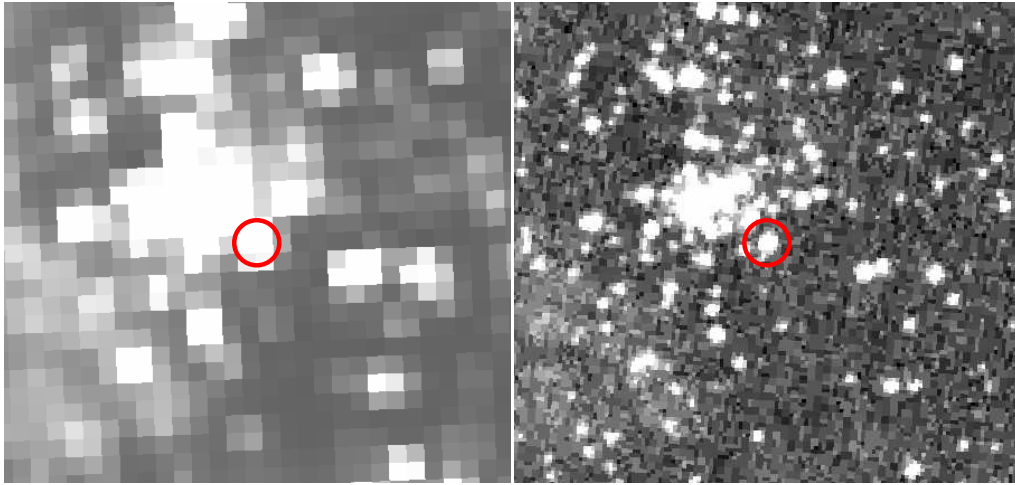
FIG. 7.— ASAS-SN (left) and DSS (right) images of the field of WR20a, where the circle around the source is $10''0$ in radius. Contamination due to the local crowding will generally distort an ASAS-SN light curve by an additive constant.
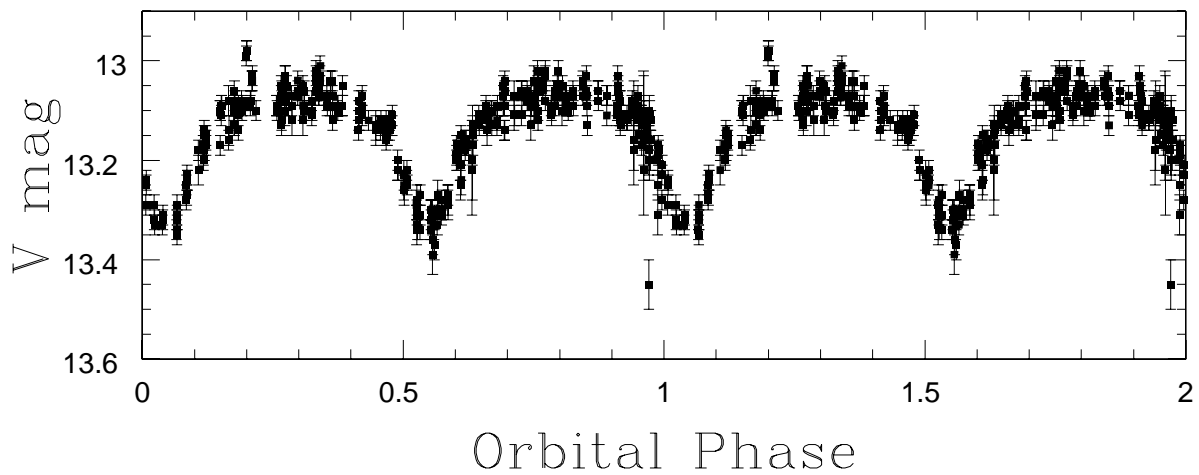
FIG. 8.— Phased ASAS-SN light curve of WR20a using the primary eclipse time of 2453124.569 from Bonanos et al. (2004) and a revised period of 3.684599 days. Blending has reduced the amplitude of the eclipses by about 0.1 mag. One bad point lies off the bottom of the figure.
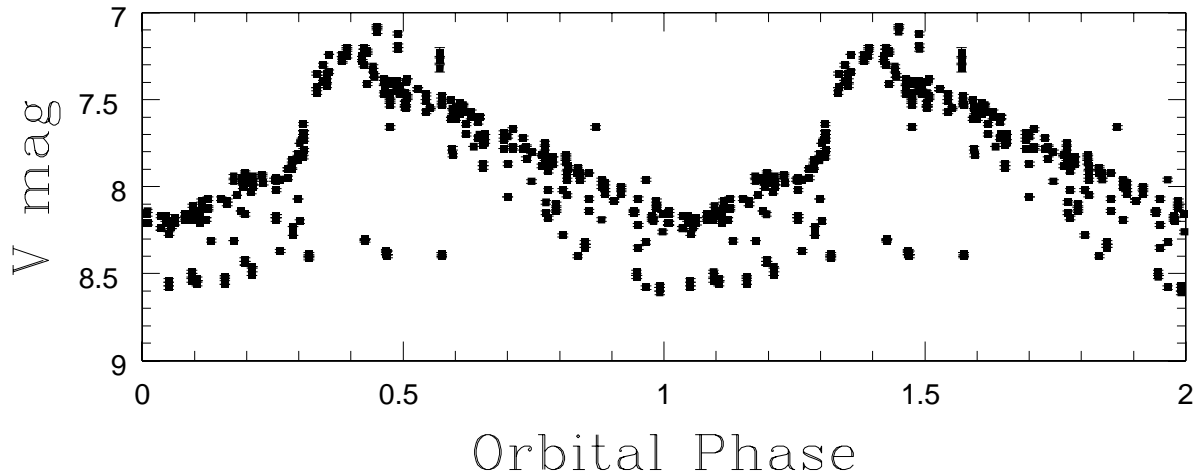
Fig. 9.— Phased ASAS-SN light curve of the bright, saturated $P = 18.9$ day Cepheid VY Car. There are 20 points that lie below 9 mag. While there are clear outliers, the light curve is surprisingly good given that the star is ~ 10 times brighter than the saturation limit. With some straightforward editing of the un-phased data, a much cleaner light curve can be constructed.

sources. Requests for recent behavior will be much faster than requests for full light curves. For one random example, it took 10, 33, 90 and 130 sec to obtain a light curve for the last 20 days, 100 days, 1000 days and the full data set, respectively. Astronomers interested in obtaining large numbers of light curves should contact the ASAS-SN team.

As outlined in the introduction, the next planned step is to provide light curves for known variables and variables newly discovered by ASAS-SN. This will be significantly faster, since the light curves will be pre-computed and stored in a database, but restricted to a particular catalog of objects. This is a well-defined process and should be completed in 2018. The full scope of the third phase, supplying light curves of sources in general, has yet to be fully determined.

REFERENCES

Aartsen, M. G., Ackermann, M., Adams, J., et al. 2017, arXiv:1702.06131
Abeysekara, A. U., Archambault, S., Archer, A., et al. 2015, ApJ, 815, L22
Boch, T., & Fernique, P. 2014, Astronomical Data Analysis Software and Systems XXIII, 485, 277
Bonanos, A. Z., Stanek, K. Z., Udalski, A., et al. 2004, ApJ, 611, L33
Bonnarel, F., Fernique, P., Bienaymé, O., et al. 2000, A&AS, 143, 33
Brown, T. M., Baliber, N., Bianco, F. B., et al. 2013, PASP, 125, 1031
Brown, J. S., Shappee, B. J., Holoien, T. W.-S., et al. 2016, MNRAS, 462, 3993
Brown, J. S., Holoien, T. W.-S., Auchettl, K., et al. 2017a, MNRAS, 466, 4904

Brown, J. S., Kochanek, C. S., Holoien, T. W.-S., et al. 2017b, arXiv:1704.02321
Davis, A. B., Shappee, B. J., Archer Shappee, B., & ASAS-SN 2015, American Astronomical Society Meeting Abstracts, 225, 344.02
De Rosa, G., Peterson, B. M., Ely, J., et al. 2015, ApJ, 806, 128
Godoy-Rivera, D., Stanek, K. Z., Kochanek, C. S., et al. 2017, MNRAS, 466, 1428
Dong, S., Shappee, B. J., Prieto, J. L., et al. 2016, Science, 351, 257
Drake, A. J., Djorgovski, S. G., Mahabal, A., et al. 2009, ApJ, 696, 870
Gully-Santiago, M. A., Herczeg, G. J., Czekala, I., et al. 2017, ApJ, 836, 200

Henden, A. A., Levine, S. E., Terrell, D., Smith, T. C., & Welch, D. 2012, Journal of the American Association of Variable Star Observers (JAAVSO), 40, 430

Herczeg, G. J., Dong, S., Shappee, B. J., et al. 2016, ApJ, 831, 133

Holoien, T. W.-S., Prieto, J. L., Stanek, K. Z., et al. 2014a, ApJ, 785, L35

Holoien, T. W.-S., Prieto, J. L., Bersier, D., et al. 2014b, MNRAS, 445, 3263

Holoien, T. W.-S., Kochanek, C. S., Prieto, J. L., et al. 2016a, MNRAS, 455, 2918

Holoien, T. W.-S., Kochanek, C. S., Prieto, J. L., et al. 2016b, MNRAS, 463, 3813

Holoien, T. W.-S., Stanek, K. Z., Kochanek, C. S., et al. 2017a, MNRAS, 464, 2672

Holoien, T. W.-S., Brown, J. S., Stanek, K. Z., et al. 2017b, MNRAS, 467, 1098

Holoien, T. W.-S., Brown, J. S., Stanek, K. Z., et al. 2017c, arXiv:1704.02320

Ivezić, Ž., Smith, J. A., Miknaitis, G., et al. 2007, AJ, 134, 973

Kato, T., Hambsch, F.-J., Monard, B., et al. 2016, PASJ, 68, 65

Lang, D., Hogg, D. W., Mierle, K., Blanton, M., & Roweis, S. 2010, AJ, 139, 1782

Law, N. M., Kulkarni, S. R., Dekany, R. G., et al. 2009, PASP, 121, 1395

Levesque, E. M., Massey, P., Żytkow, A. N., & Morrell, N. 2014, MNRAS, 443, L94

Littlefield, C., Garnavich, P., Kennedy, M. R., et al. 2016, ApJ, 833, 93

Lubin, J. B., Rodriguez, J. E., Zhou, G., et al. 2017, arXiv:1706.02401

Osborn, H. P., Rodriguez, J. E., Kenworthy, M. A., et al. 2017, arXiv:1705.10346

Paczyński, B. 2000, PASP, 112, 1281

Pojmanski, G. 2002, Acta A., 52, 397

Rodriguez, J. E., Stassun, K. G., Cargile, P., et al. 2016, ApJ, 831, 74

Rodriguez, J. E., Zhou, G., Cargile, P. A., et al. 2017, ApJ, 836, 209

Schmidt, S. J., Prieto, J. L., Stanek, K. Z., et al. 2014, ApJ, 781, L24

Schmidt, S. J., Shappee, B. J., Gagné, J., et al. 2016, ApJ, 828, L22

Shappee, B. J., Prieto, J. L., Grupe, D., et al. 2014, ApJ, 788, 48

Stanek, K. Z., Kochanek, C. S., Brown, J. S., et al. 2016, The Astronomer's Telegram, 9669

Udalski, A., Szymanski, M. K., Soszynski, I., & Poleski, R. 2008, Acta A., 58, 69

Woźniak, P. R., Vestrand, W. T., Akerlof, C. W., et al. 2004, AJ, 127, 2436